https://doi.org/10.5194/tc-2019-188
Preprint. Discussion started: 4 September 2019

The Cryosphere Discussions
Open Access
EGU

Remapping of Greenland ice sheet surface mass balance anomalies for large ensemble sea-level change projections

Heiko Goelzer[1,2], Brice P. Y. Noel[1], Tamsin L. Edwards[3], Xavier Fettweis[4], Jonathan M. Gregory[5,6], William H. Lipscomb[7], Roderik S. W. van de Wal[1,8], Michiel R. van den Broeke[1]

(1) Institute for Marine and Atmospheric research Utrecht, Utrecht University, Utrecht, the Netherlands
(2) Laboratoire de Glaciologie, Université Libre de Bruxelles, Brussels, Belgium
(3) Department of Geography, King's College, London, UK
(4) Laboratory of Climatology, Department of Geography, University of Liège, Liège, Belgium
(5) National Center for Atmospheric Science, University of Reading, Reading, UK
(6) Met Office, Hadley Centre, Exeter, UK.
(7) Climate and Global Dynamics Laboratory, National Center for Atmospheric Research, Boulder, CO, USA
(8) Geosciences, Physical Geography, Utrecht University, Utrecht, the Netherlands

Correspondence to: Heiko Goelzer (h.goelzer@uu.nl)

Abstract

Future sea-level change projections with process-based standalone ice sheet models are typically driven with surface mass balance (SMB) forcing derived from climate models. In this work we address the problems arising from a mismatch of the modelled ice sheet geometry with the one used by the climate model. We present a method to apply SMB forcing from climate models to a wide range of Greenland ice sheet models with varying and temporally evolving geometries. In order to achieve that, we translate a given SMB anomaly field as a function of absolute location, to a function of surface elevation for 25 regional drainage basins, which can then be applied to different modelled ice sheet geometries. The key feature of the approach is the non-locality of this remapping process. The method reproduces the original forcing data closely when remapped to the original geometry. When remapped to different modelled geometries it produces a physically meaningful forcing with smooth and continuous SMB anomalies across basin divides. The method considerably reduces non-physical biases that would arise by applying the SMB anomaly derived for the observed geometry directly to a large range of modelled ice sheet model geometries.

https://doi.org/10.5194/tc-2019-188
Preprint. Discussion started: 4 September 2019


The Cryosphere Discussions

1 Introduction

Process-based ice sheet model projections are an important tool to estimate future sea-level change in the context of the Intergovernmental Panel on Climate Change assessment cycle (IPCC, 2013). For the first time, in the upcoming IPCC assessment report (AR6), ice sheet model projections are formally embedded in the Coupled Model Intercomparison Project (CMIP, Eyring et al., 2016) in the form of the CMIP-endorsed Ice Sheet Model Intercomparison Project ISMIP6 (Nowicki et al., 2016). ISMIP6 aims at providing estimates of the future sea-level contribution from the Greenland and Antarctic ice sheets based on standalone ice sheet model (ISM) simulations, forced by output from CMIP atmosphere-ocean global climate models (GCMs) and fully-coupled ISM-GCMs. This paper focuses on standalone simulations of the Greenland ice sheet (GrIS).

The first ISMIP6 activities focused mainly on the problem of ice sheet model initialisation (Goelzer et al., 2018a; Seroussi et al., 2019), but also identified issues that may be encountered when a large range of ice sheet models is forced with climate model output. The most important forcing derived from climate models in the context of future sea-level change projections for the GrIS is the surface mass balance (SMB) describing the amount of mass that is added or removed at the ice sheet surface. For the ISMIP6 projections it was decided to apply the SMB forcing as an anomaly, i.e. as the change in SMB relative to a given reference period. This approach has the important advantage that it allows for participating ice sheet modellers to use their own SMB product during initialisation and simply add provided SMB anomalies in a projection experiment.

However, problems were identified when a given surface mass balance anomaly (aSMB) was applied to the wide range of Greenland ice sheet models used in the community (Goelzer et al., 2018a). The key issue is a mismatch between modelled initial and observed ice sheet geometries, related to uncertainties in forcing, physical parameters, and the underlying model physics. For instance, a geometrical mismatch generally means that the modelled ablation zone and the prescribed anomalous ablation are not co-located, leading to an incorrect mass balance forcing.

With the original intention to apply identical forcing to all participating models, a forcing data set was prepared for initMIP-Greenland (Goelzer et al., 2018a) that consisted of an SMB anomaly based on the present-day observed geometry. The SMB anomaly was extended outside the observed ice sheet mask following a simple parameterization to accommodate larger than observed ice sheet model extents. In practice, however, ice sheet models with larger-than-observed initial areas exhibit larger melting under such forcing, simply because their ablation areas are extended outwards.

To solve this problem, we present here a method to remap the SMB anomaly as a function of surface elevation, and thereby produce appropriate forcing for different ice sheet model geometries. The proposed method was developed for future sea-level change projections made with a large ensemble of ice sheet models (with possibly widely different initial geometries) forced by output of different climate models and scenarios. However, other applications can be envisioned, for example any other case where the climate model forcing is generated for an ice sheet geometry differing from that of the ice sheet model itself.

https://doi.org/10.5194/tc-2019-188
Preprint. Discussion started: 4 September 2019

Asynchronously-coupled climate-ice sheet simulations and experiments with accelerated climatic boundary conditions may also be improved with the presented method.

In the following we describe our approach and method (Sec 2), the resulting forcing (Sec 3), and time dependent applications (Sec 4), and finally discuss the results (Sec 5).

2 Approach and method

Our approach aims to generate an SMB forcing (at a yearly time scale) applicable to an ensemble of Greenland ice sheet models that exhibit a wide range of initial present-day ice sheet geometries. The forcing is based on an existing aSMB product that is generated at a fixed surface elevation based on present-day observations. This aSMB product will typically be the output of a regional climate model, but could come from any SMB model or GCM. While the forcing will have to be adapted for the individual model geometries, it should remain as similar as possible to the original product when applied to the observed present-day geometry.

The proposed method is based on the strong elevation dependence of SMB and aSMB and is illustrated for a schematic flowline of a land-terminating ice sheet margin (Figure 1). For a larger ice sheet geometry (red, dashed), the horizontal equilibrium line position lies farther from the ice divide than for a smaller ice sheet (black). It is this effect that we are trying to capture with our method. Remapping the SMB anomaly as a function of surface elevation, as we propose, allows for a "stretching" of the SMB product to match the larger ice sheet extent, while maintaining its overall structure.

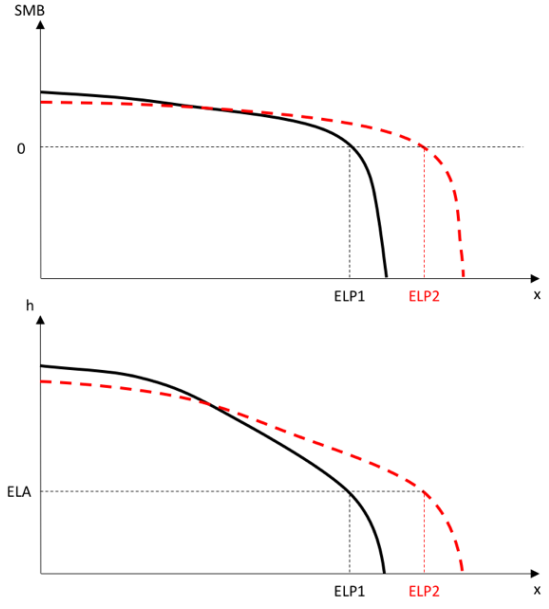

Figure 1 Schematic cross section for two different ice sheet geometries (bottom) and associated surface mass balance (top). The two geometries share the same equilibrium line altitude (ELA), but exhibit different horizontal equilibrium line positions (ELP1, ELP2).

https://doi.org/10.5194/tc-2019-188
Preprint. Discussion started: 4 September 2019

For initMIP-Greenland, the SMB anomaly was parameterised as a fixed function of observed surface elevation and latitude (Goelzer et al., 2018a), which was subsequently used to define a forcing product everywhere on the grid. In principle, we could use the same global approach to generate SMB forcing for a range of different initial ice sheet geometries. However, regional differences in the height-aSMB relationship can be large and justify a spatially better resolved approach.

To capture regional differences, we therefore apply the remapping for a set of drainage basins (Shepherd et al., 2012; Zwally et al., 2012; Mouginot et al. 2019). In practice, the following steps are executed to (1) derive and (2) apply the height-aSMB relationship to different geometries.

(1) Defining an elevation-aSMB lookup table:

- Divide the ice sheet into drainage basins
- For each individual drainage basin do:
    - For each elevation band with central height h_c and range R of heights do:
        - find aSMB values for all heights in R
        - calculate the median aSMB of these
        - Save result to lookup table aSMB=f(h_c)

(2) Remap aSMB to a new geometry:

- Use the drainage basins separation in (1)
- For each individual drainage basin do:
    - For each ISM grid point do:
        - interpolate aSMB linearly as a function of height using a combination of lookup tables (1) for this and neighbouring basins (see Sec 2.2)

2.1 Defining an elevation-aSMB lookup table

The first step (defining an elevation-aSMB lookup table) is independent of the ice sheet model characteristics and relies only on the initial aSMB product, the climate model's surface elevation field, and a meaningful basin selection. Ideally, the basin division should separate regions with largely different SMB characteristics, e.g. wet and dry regions. At the same time, our method requires that each basin contains a wide elevation range so that the lookup tables can be completely filled. For this study we created 25 basins by combining several smaller basins from a recent drainage delineation (Mouginot et al. 2019). The basins may consist only of single outlet glaciers or even flowlines, as long as they cover a sufficiently large elevation range. The basin delineation is extended outside the observed ice sheet mask to accommodate different (i.e. larger) ice sheet geometries than observed (Figure 2). This was done once manually using observed topography of ice-free regions and bathymetry as guidance.

While the method can be applied to any aSMB product, here we use model output from the regional climate model MAR (Fettweis et al., 2013), as it has been run for the RCP8.5 scenario and was chosen for ISMIP6. We use output of MAR version 3.9 run at a horizontal resolution of 15 km that has been extrapolated to 1 km resolution. (Delhasse et al., 2019). We

https://doi.org/10.5194/tc-2019-188
Preprint. Discussion started: 4 September 2019

demonstrate the method here with aSMB at the end of the century relative to the present day, calculated as the time mean change:

$$aSMB = \overline{SMB}^{2096-2100} - \overline{SMB}^{2006-2010}. \quad (1)$$

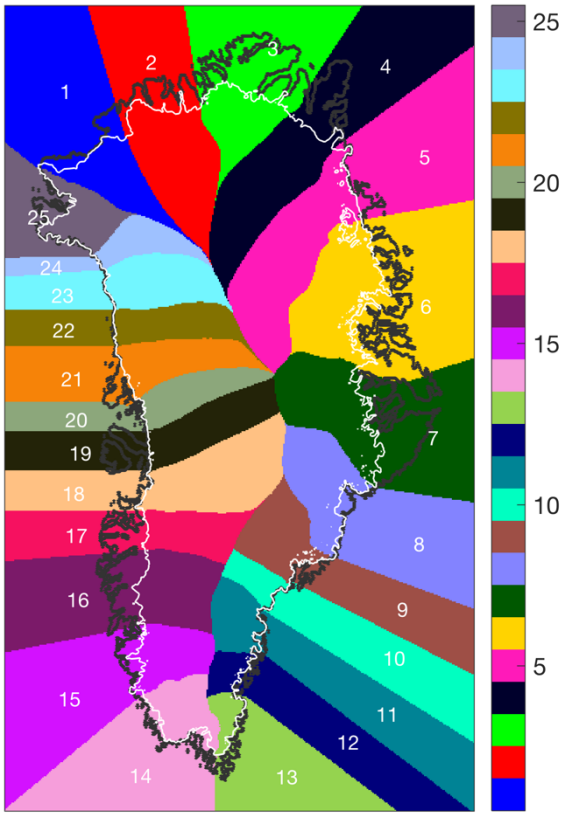

Figure 2 Basin separation. The basin delineation is based on Mouginot et al. (2019), combined into a set of 25 regional basins and extended to the grid margin.

For each drainage basin we define an elevation-aSMB lookup table based on the MAR SMB data in that basin. We define elevation bands with centre h_c and range R, find all grid points with matching elevation, and register the associated aSMB values. We calculate the median aSMB value of all available points for each elevation band (Figure 3), resulting in a lookup table aSMB=f(hc). The step size dh=100 m between subsequent h_c and the value of R=100 m was chosen after some initial testing, but was not formally optimised. It was judged sufficient to describe the variation in the elevation-aSMB relationships for each basin (Figure 3). Other interval sizes may be more appropriate for other climate forcing products.

https://doi.org/10.5194/tc-2019-188
Preprint. Discussion started: 4 September 2019

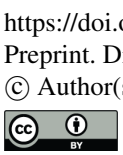

For all basins we copied the table entry at 100 m to 0 m, rather than using the 0-50 m height interval with sparser data. For basins with missing values for high elevations, we repeated the highest-elevation aSMB value until 3500 m (circles in Figure 3).

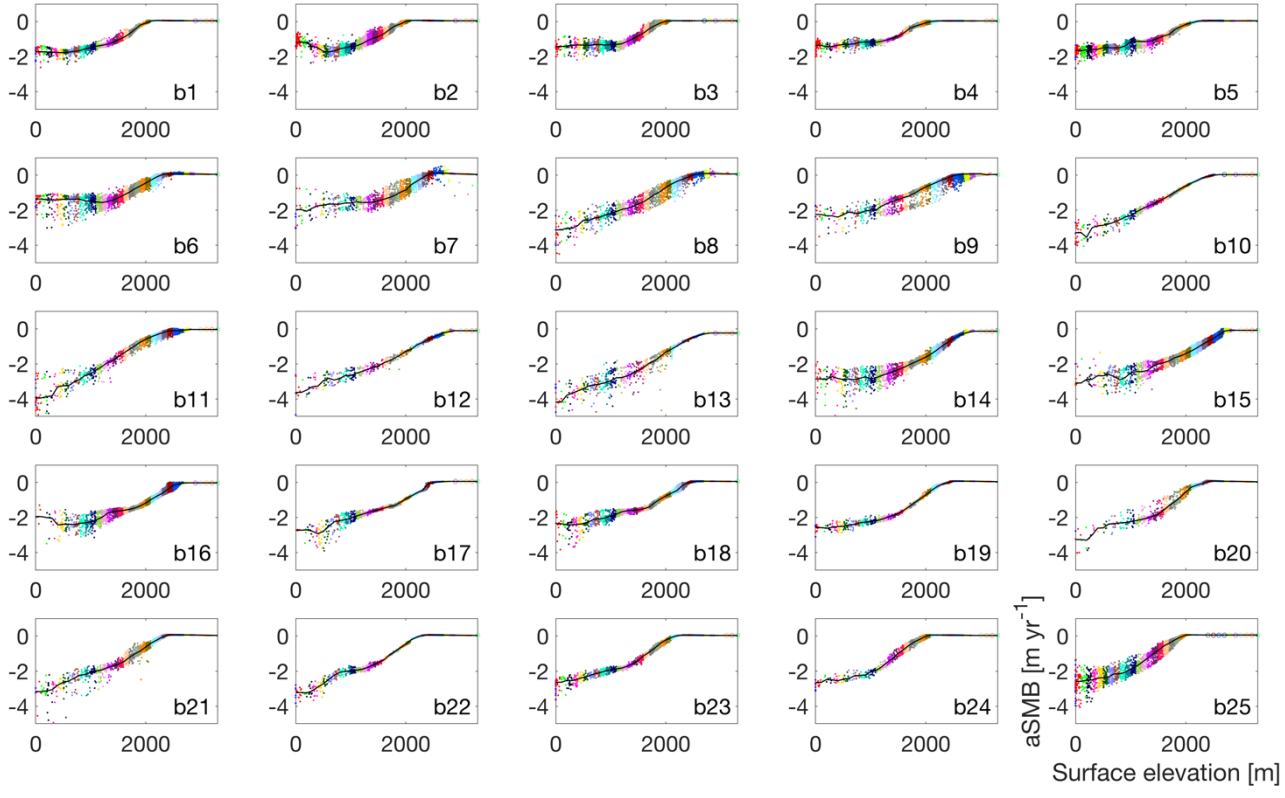

Figure 3 SMB anomaly (m ice equivalent per year) from the RCM MAR (scatter) and with the elevation interval medians (used for the mapping) shown with a black line. Different colours indicate the elevation ranges considered for the elevation-aSMB lookup table.

2.2 Remap aSMB to a new geometry

For the reconstruction of SMB on an ice sheet model geometry, we define the aSMB for each grid point using a combination of lookup tables from the local and neighbouring basins. We weight the aSMB values of the surrounding neighbour basins by proximity, which results in a gradual decrease of influence of the next neighbouring basin away from the divides (Figure 4). The aSMB for each point in a specific basin b_0 is calculated as

$$aSMB_{b0}(x,y) = \mathrm{aSMB}_{b0}(h) * \mathrm{w}_0(x,y) + \mathrm{aSMB}_{b1}(h) * \mathrm{w}_1(x,y) + \ldots \mathrm{aSMB}_{bn}(h) * \mathrm{w}_n(x,y), \quad (2)$$

where $\mathrm{aSMB}_{bi}(h)$ is the aSMB value found by interpolating the lookup table for basin b_i at the elevation h(x,y).

https://doi.org/10.5194/tc-2019-188
Preprint. Discussion started: 4 September 2019

The weights of the gradients in the current basin b_0, are calculated as

$$w_0 = 1 - \frac{p_1+p_2+\cdots+p_n}{p_0+p_1+p_2+\cdots+p_n}, \quad (3)$$

which is the residual of the sum of the weights for neighbouring basins b_1 through b_n defined as

$$w_1 = \frac{p_1}{p_0 + p_1 + p_2 + \cdots + p_n} \quad (4)$$

...

$$w_n = \frac{p_n}{p_0+p_1+p_2+\cdots+p_n}.$$

Here p_0=1 and p_1, p_2, … p_n are proximities of a given point to the neighbouring basins b_1- b_n which are limited to the interval [0, 1]:

$$p_i = 1 - \min\left(\frac{ds_i}{ds_{norm}}, 1\right), \quad (5)$$

where ds_i is the distance from a given point in b_0 to the nearest point in neighbouring basin b_i, which is normalized by a prescribed distance $ds_{norm} = 50\ km$. This value of ds_{norm} was chosen to minimize the mismatch between original and reconstructed aSMB (other tested values were 75, 100 and 125 km), though variations in ds_{norm} have limited influence on the results. As an example, near divides with only one neighbouring basin in proximity, the local weighting factor w_0 increases from 0.5 at the divide to 1.0 at the centre of the basin (Figure 4).

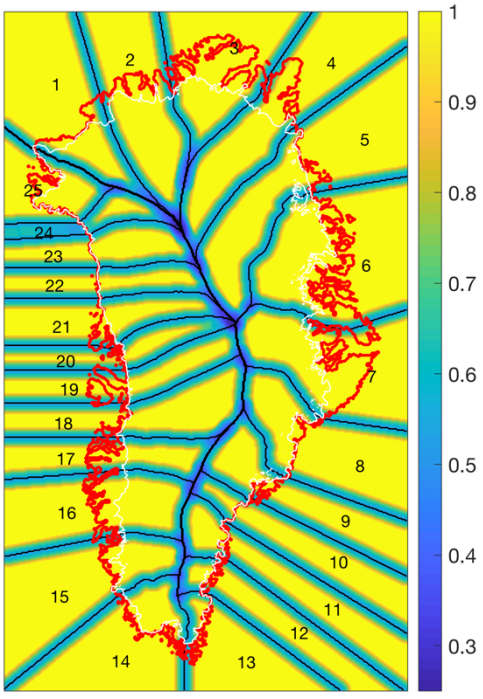

Figure 4 Weighting factor of the local basin for remapping. The local weighting factor increases from the basin divides (black lines) to 1.0 in the centre over a specified distance (here 50 km), while the factor for the neighbouring basin decreases proportionally (not shown).

https://doi.org/10.5194/tc-2019-188
Preprint. Discussion started: 4 September 2019

The Cryosphere Discussions
Open Access
EGU

3 Results

Figure 5 shows results for aSMB at the end of the MAR RCP8.5 simulation (Eq. 1). The original MAR aSMB (Fig. 5a) has been used to remap aSMB at the same surface elevation (Fig. 5b).

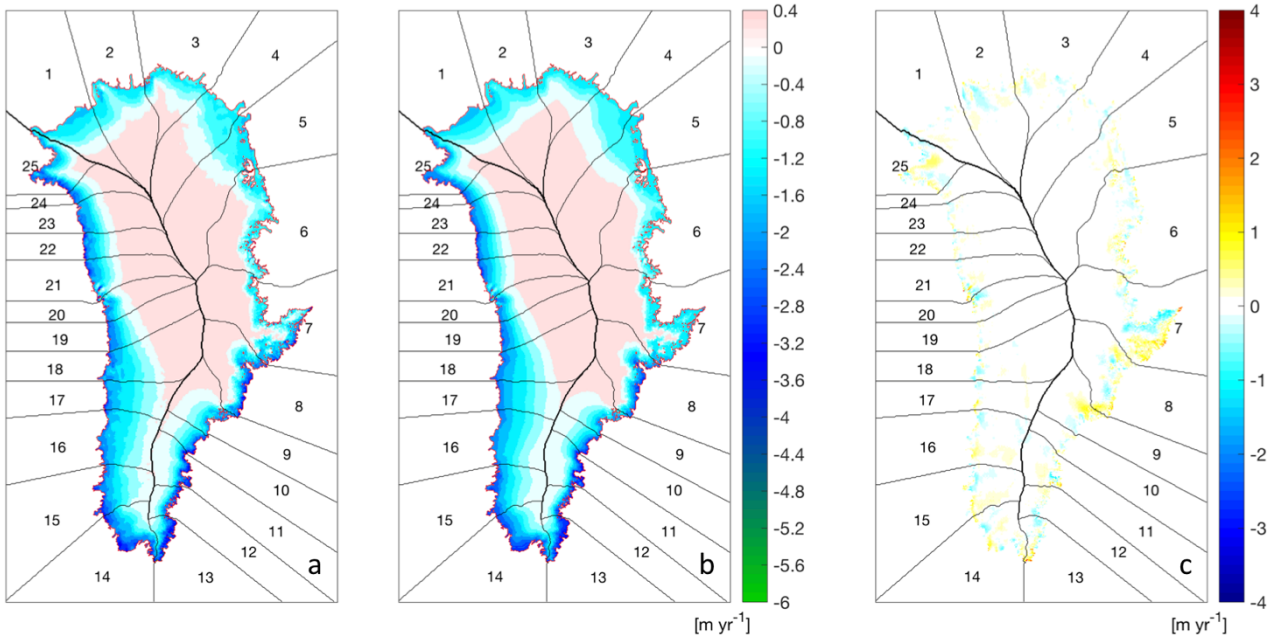

Figure 5 SMB anomaly from the RCM MAR for the observed geometry (a), remapped to the same observed geometry (b) and differences b-a (c).

The reconstructed aSMB is very similar to the original, reproducing the overall pattern. Some smaller-scale features are lost, however, by averaging laterally across the basin and over elevation bands. The absolute error in spatially integrated aSMB per region is in this case on average 2.3% with extremes of 4%, 7% and 15% in basins 7, 8 and 9, respectively (Figure 6). We consider this acceptable given typical uncertainties in climate model forcing (e.g. van den Broeke et al., 2017) and our specific interest in large scale, ice-sheet-wide results to be used in ISMIP6.

https://doi.org/10.5194/tc-2019-188
Preprint. Discussion started: 4 September 2019

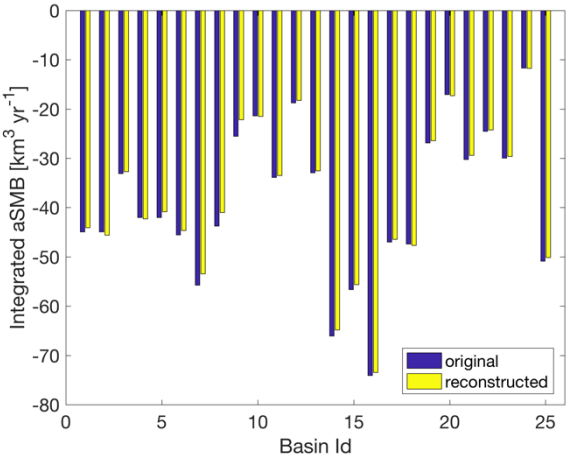

Figure 6 Integrated aSMB per basin from original MAR model output (blue) and for reconstruction on the same geometry (yellow).

The remapped aSMB for an example modelled geometry with large differences relative to the observed is shown in Figure 7c for one member of the initMIP ensemble (VUB_GISM). The remapped aSMB shows a pattern similar to the original (Figure 7a) with smooth and continuous aSMB across basin divides. Where the ice sheet extends well beyond the observed ice mask (red contour lines) the aSMB is naturally extended following the modelled surface elevation, as is best visible in sector 3. Results from a standard method of extending the SMB outside the observed ice sheet mask at the observed surface elevation (Franco et al., 2012) are shown in Figure 7b for the footprint of the modelled ice sheet. This method uses the 4 closest, distance-weighted SMB values inside the MAR ice mask, and applies a correction based on the elevation difference between the interpolated elevation of the 4 SMB pixels and the local elevation by using the local vertical SMB gradient computed in this area. Due to low elevation of the tundra surrounding the ice sheet, the extension provides generally low aSMB for regions outside the observed ice sheet mask, which is illustrated in Figure 7d, showing the difference between the original (Figure 7a) and extended (Figure 7b) aSMB. By definition, the original and extended aSMB are identical over the common ice mask, but positive differences can be seen in regions where the modelled ice sheet is smaller (Figure 7d). The remapping method notably prevents the occurrence of large-amplitude negative aSMB outside of the observed ice sheet mask, illustrated by the difference between the two approaches (Figure 7e).

We quantify the differences between the three aSMB products again by integrating them over the drainage basins (Figure 8a). The largest differences between the original and extended aSMB are found in basins where the modelled ice sheet extends far beyond the observed ice sheet mask (basins 3, 4 ,6 and 7), or where the aSMB has large negative amplitude (basin 12, 14 and 15). In all these cases, the remapping reduces the bias (in most cases considerably), which is visualised showing basin integrals of differences between original and extended (blue) and between extended and remapped aSMB (yellow) in Figure 8b. In most cases, biases in the extended aSMB (blue) are reduced by the remapping, illustrated by bars of opposite sign (yellow).

https://doi.org/10.5194/tc-2019-188
Preprint. Discussion started: 4 September 2019

The biases are reduced but are not expected to be entirely removed by the remapping, because a physically larger ice sheet should have a larger ablation area. The improvement of the aSMB forcing by the remapping is mainly found in regions where the modelled ice sheet extends beyond the observed mask and where the remapped aSMB is predominantly higher than the extended aSMB (Figure 7e). Differences between original and remapped aSMB in the interior of the ice sheet (Figure 7e) indicate averaging in the remapping process as discussed before, but more importantly are due to differences in the modelled surface elevation compared to the observed. This illustrates a feature of the remapping method that can be interpreted both as an asset or as a shortcoming, namely that biases in surface elevation (Figure 7f) are propagated to the aSMB forcing.

For ice sheet models with initial states close to observations, the reconstructed aSMB looks very similar to the original, while for models with largely different geometry, the overall structure of decreasing aSMB towards lower elevation is well captured. A similar comparison as in Figure 7c and Figure 8a, for three other modelled geometries from the initMIP-Greenland ensemble is given in the supplement (Figure S1 and Figure S2).

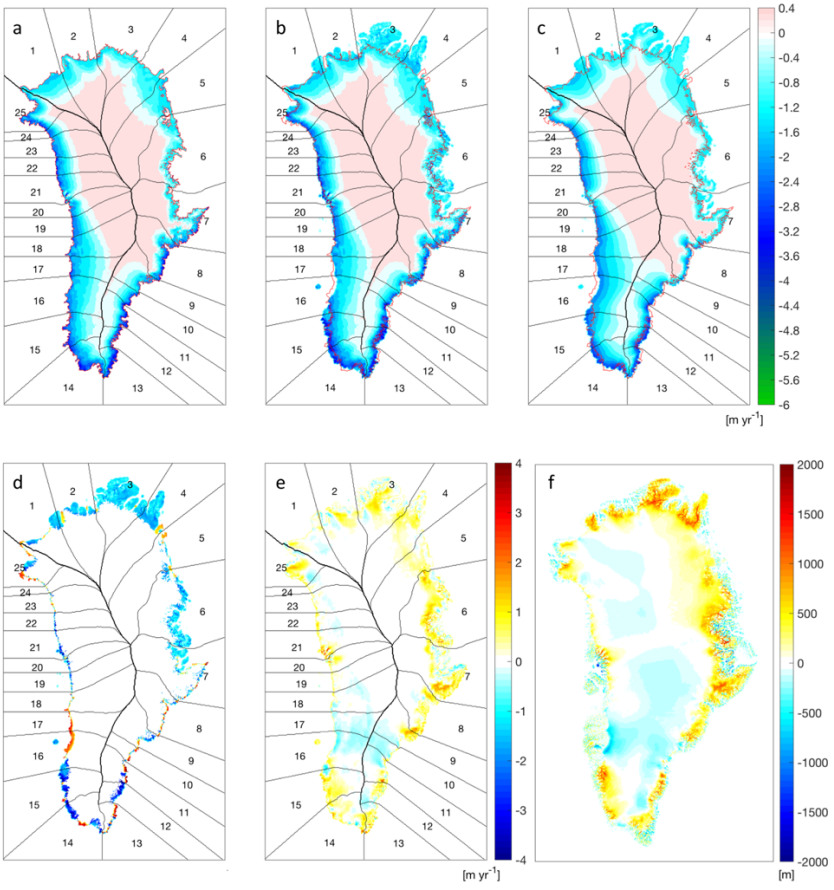

Figure 7 (a) SMB anomaly from the RCM MAR (same as Figure 5a), (b) extended to the VUB_GISM initial geometry using the method of Franco at al. (2012), (c) remapped with weighting between neighbouring basins for the same geometry, (d) difference b-a, (e) difference c-b and (f) model bias in surface elevation.

https://doi.org/10.5194/tc-2019-188
Preprint. Discussion started: 4 September 2019

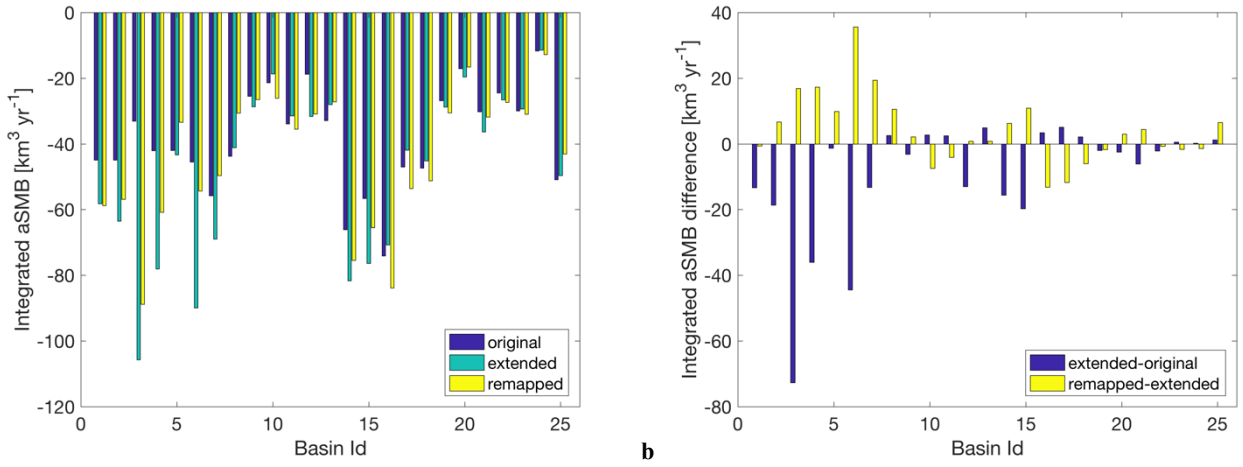

a b

Figure 8 Remapping results for a model state far from the observed geometry. (a) Integrated aSMB per basin from MAR model output on the observed ice mask (blue), for extension of the VUB_GISM model ice mask (green) and remapped to the VUB_GISM model geometry (yellow). (b) Differences between extended and original aSMB (blue) and between remapped and extended aSMB (yellow).

4 Time dependent forcing

The same method can be used to define elevation-aSMB lookup tables and calculate remapped aSMB for climate change scenarios, generating a time-dependent forcing. We have done this as a pilot application for MARv3.9 forced by MIROC5 (Watanabe et al. 2010) under scenario RCP8.5 (Figure 9) with available SMB data from 1995-2100 (Fettweis et al., 2013; Delhasse et al., 2019) computed for ISMIP6. We have calculated aSMB for the period 2015-2100 against a reference SMB as an average of the period 1995-2014. The resulting lookup tables (Figure 9) show the decrease in aSMB for the lower parts of each basin as expected.

https://doi.org/10.5194/tc-2019-188
Preprint. Discussion started: 4 September 2019

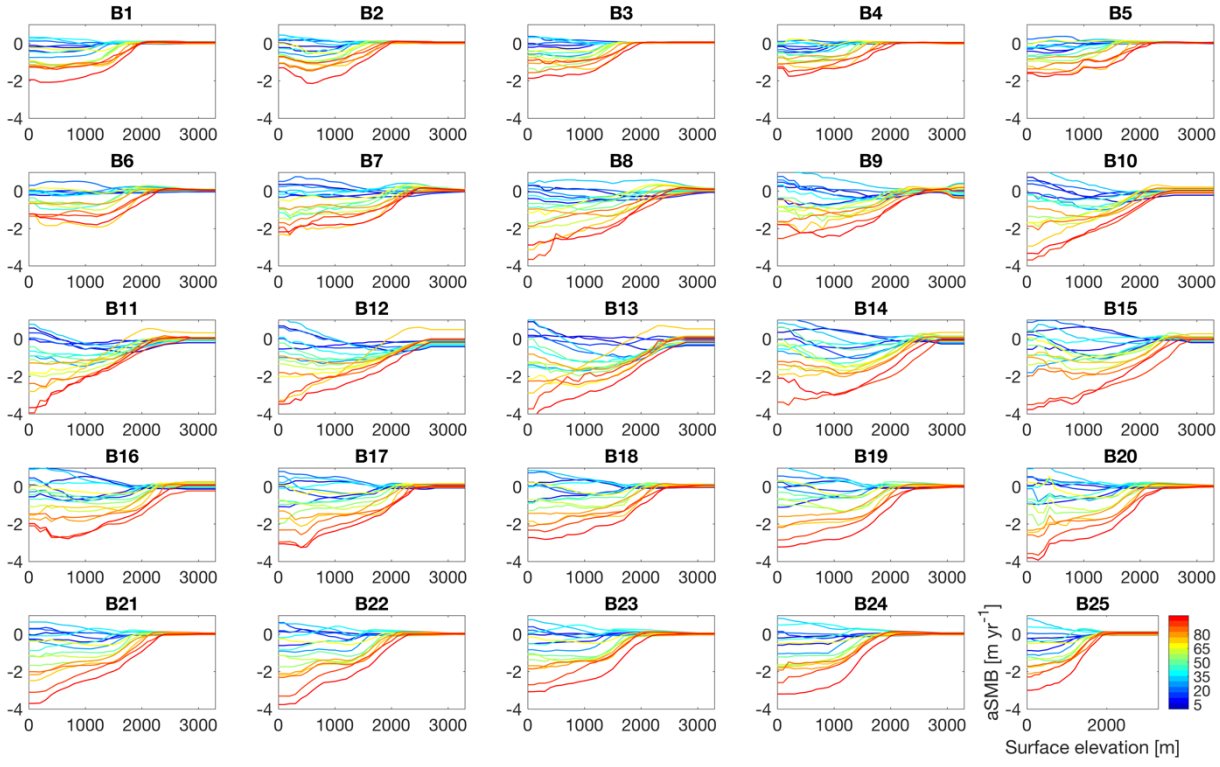

Figure 9 Elevation-aSMB lookup tables for climate change scenario MAR MIROC5 RCP8.5. Time is colour coded to indicate years since 2015 with lines given every 5 years until year 2100.

4.1 Future sea-level change projections

The initial goal of the proposed method was to apply it to future sea-level change projections with a large ensemble of ice sheet models (with possibly widely different initial geometries) and forced by output of different climate models and scenarios, e.g. in the framework of the ice sheet model intercomparison project ISMIP6 (Nowicki et al., 2016; Goelzer et al., 2019). For such applications, the basin separation can be defined and the lookup tables can be calculated for specific climate models and scenarios ahead of time. Basin separation and weighting functions can be calculated for each specific ice sheet grid in advance. To apply a specific forcing scenario, the information transmitted to an individual ice sheet modeller consists of aSMB values for L elevation bands for M basins at N time steps. When the initial ice sheet geometries are known in advance, the remapping can also be done offline and aSMB(x,y,t) can be distributed directly, avoiding the need to implement the remapping in each individual ice sheet model (see section 2.2).

To test the feasibility of our method, we have applied it to a projection using only modelled and remapped aSMB to infer changes in ice sheet geometry. By ignoring any ice dynamic adjustment (i.e. no ice sheet model is used) and assuming the ice sheet to be in steady state with an unknown reference SMB, the time evolution of the ice sheet is fully determined by the initial

https://doi.org/10.5194/tc-2019-188
Preprint. Discussion started: 4 September 2019

geometry (surface elevation and mask) and the given aSMB. This setup does not consider any ice dynamic effects, such as the adjustment of ice flow to the SMB change itself and variations in marine terminating outlet glaciers. We emphasize that this experimental setup serves to illustrate the use of the remapping method and should not be interpreted as a real projection.

We first compare two different representations of the cumulative (time-integrated) SMB anomaly as a measure of the spatially resolved ice thickness change at the end of the scenario.

1. The time-integrated original aSMB of the climate model, by definition at fixed surface elevation (MOD).
2. The time-integrated aSMB calculated by remapping to a fixed surface elevation (MAP).

In both cases, the resulting thickness change for aSMB<0 is limited by the available ice thickness at each grid point.

The two cases MOD and MAP show similar results (Figure 10a,b), indicating that the remapping performs well to capture the general pattern of SMB change also in this time-dependent application. Direct comparison between MOD and MAP (Figure 10c) reveal limitations in the remapping, mainly arising from localised melt and precipitation anomalies that are not resolved with 25 basins or where the relationship between surface elevation and aSMB breaks down (see also Figure 5c). The difference map (Figure 10c) shows some along-flow features on a larger spatial scale, suggesting that further refinement of the regions could improve the representation.

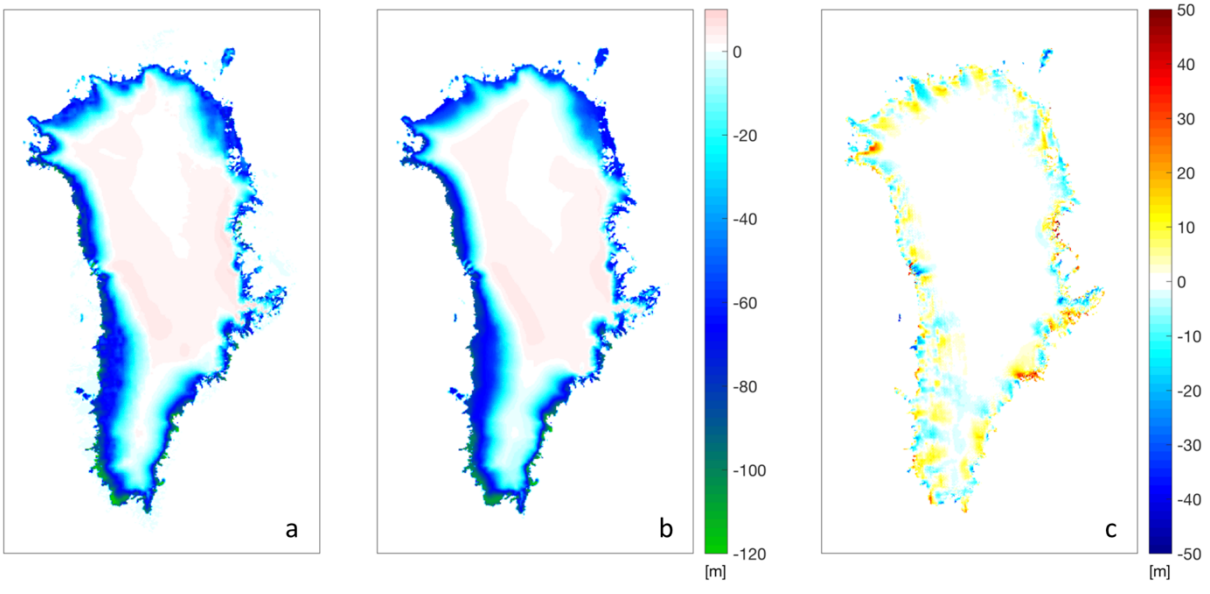

Figure 10 Time-integrated aSMB for MOD (a), MAP (b) and differences MAP-MOD (c), representing the error of the remapping.

4.2 SMB-height feedback

In general the SMB anomaly aSMB(t, h) that should be applied at any point on the evolving ice-sheet surface h depends both explicitly on time t, because the climate is changing, and implicitly on time, because the geometry h(t) is changing. We denote

https://doi.org/10.5194/tc-2019-188
Preprint. Discussion started: 4 September 2019


The Cryosphere Discussions

the height by $\overline{\mathrm{h}}$ for the SMB anomaly and other quantities calculated from the RCM output at a fixed surface elevation, by $h_0 = \mathrm{h}(0)$ when remapping to the initial surface elevation that the ice-sheet has at $\mathrm{t} = 0$, and by $\mathrm{h} = \mathrm{h}(\mathrm{t})$ when remapping to a time evolving geometry. The SMB anomaly in the RCM (at fixed surface elevation $\overline{\mathrm{h}}$) can then be expressed as $\mathrm{aSMB}(\mathrm{t}) = \mathrm{SMB}(\mathrm{t}) - \mathrm{SMB}(0)$ and the changes of SMB and aSMB with surface elevation by $\mathrm{d}(\mathrm{SMB}(\mathrm{t}))/\mathrm{dz}$ and $\mathrm{d}(\mathrm{aSMB}(\mathrm{t}))/\mathrm{dz}$, respectively. The latter can be written as

$$\mathrm{d}(\mathrm{aSMB}(\mathrm{t}))/\mathrm{dz} = \mathrm{d}(\mathrm{SMB}(\mathrm{t}))/\mathrm{dz} - \mathrm{d}(\mathrm{SMB}(0))/\mathrm{dz}, \quad (6)$$

where the term d(SMB)/dz(t) can be approximated from the RCM output, typically by analysing spatial SMB gradients in close proximity of the point of interest (Franco et al., 2012; Noël et al., 2016; Le clec'h et al., 2019), or by parameterising the effect (e.g. Edwards et al., 2014a,b; Goelzer et al, 2013).

The remapping of a quantity X from the fixed surface elevation $\overline{\mathrm{h}}$ to h is formally written as operator $\mathrm{R}\left(\mathrm{X}\left(\mathrm{t}, \overline{\mathrm{h}}\right), \mathrm{h}\right)$, where we will omit parameter $\overline{\mathrm{h}}$ in the following for clarity. If we remapped the time-evolving aSMB(t) from the fixed RCM topography to the initial ice-sheet topography, as in the test procedure of Section 4.1, we would only include the climate-dependence of aSMB (its explicit dependence on time), but omit the effect of changing surface elevation (the implicit dependence on time). If instead we remap $\mathrm{aSMB}\left(\mathrm{t}, \overline{\mathrm{h}}\right)$ to the evolving h(t), we include a dependence on the modelled elevation change $\mathrm{dh}(\mathrm{t}) = \mathrm{h}(\mathrm{t}) - h_0$, and the remapping can be approximated as

$$\mathrm{R}(\mathrm{aSMB}(\mathrm{t}), \mathrm{h}) \approx \mathrm{aSMB}(\mathrm{t}) + \mathrm{d}\left(\mathrm{aSMB}(\mathrm{t})\right)/\mathrm{dz} * \mathrm{dh}(\mathrm{t}). \quad (7)$$

By using (6), we get the quantity

$$\delta\mathrm{SMB}(\mathrm{t}, \mathrm{h}) \approx \mathrm{aSMB}(\mathrm{t}) + [\mathrm{d}(\mathrm{SMB}(\mathrm{t}))/\mathrm{dz} - \mathrm{d}(\mathrm{SMB}(0))/\mathrm{dz}] * \mathrm{dh}(\mathrm{t}) \quad (8)$$

(shown in **Figure 11**c). This quantity however includes only the elevation-dependence of the time-dependence of SMB, which is a second-order effect, and it omits the first-order effect of the height feedback on SMB.

The SMB anomaly that should be applied to the evolving ice-sheet includes both effects, and can be written as

$$\mathrm{aSMB}(\mathrm{t}, \mathrm{h}) \equiv \mathrm{R}(\mathrm{SMB}(\mathrm{t}), \mathrm{h}) - \mathrm{R}(\mathrm{SMB}(0), \mathrm{h}_0) \quad (9)$$

$$= \mathrm{R}(\mathrm{SMB}(\mathrm{t}), \mathrm{h}_0) - \mathrm{R}(\mathrm{SMB}(0), \mathrm{h}_0) + \mathrm{R}(\mathrm{SMB}(\mathrm{t}), \mathrm{h}) - \mathrm{R}(\mathrm{SMB}(\mathrm{t}), \mathrm{h}_0)$$

$$\mathrm{aSMB}(\mathrm{t}, \mathrm{h}) \approx \mathrm{R}(\mathrm{aSMB}(\mathrm{t}), \mathrm{h}_0) + \mathrm{R}(\mathrm{d}(\mathrm{SMB}(\mathrm{t}))/\mathrm{dz}, \mathrm{h}_0) * \mathrm{dh}(\mathrm{t}). \quad (10)$$

Comparing (8) and (10), we can appreciate that (8) is incomplete because the first term in square brackets, which also appears in (10), is mostly cancelled by the second term in square brackets; indeed, if the vertical gradient of SMB is the same in the two climates, there is no effect of elevation change in (8). To calculate (10), thus preserving the full effect of elevation change on aSMB, we remap the time-dependent $\mathrm{aSMB}\left(\mathrm{t}, \overline{\mathrm{h}}\right)$ and $\mathrm{d}(\mathrm{SMB}\left(\mathrm{t}, \overline{\mathrm{h}}\right))/\mathrm{dz}$ to the initial ice-sheet topography h_0.

An alternative method of calculation is suggested by writing

$$\mathrm{aSMB}(\mathrm{t}, \mathrm{h}) \equiv \mathrm{R}(\mathrm{SMB}(\mathrm{t}), \mathrm{h}) - \mathrm{R}(\mathrm{SMB}(0), \mathrm{h}_0) \quad (11)$$

$$= \mathrm{R}(\mathrm{SMB}(\mathrm{t}), \mathrm{h}) - \mathrm{R}(\mathrm{SMB}(0), \mathrm{h}) + \mathrm{R}(\mathrm{SMB}(0), \mathrm{h}) - \mathrm{R}(\mathrm{SMB}(0), \mathrm{h}_0)$$

$$\mathrm{aSMB}(\mathrm{t}, \mathrm{h}) \approx \mathrm{R}(\mathrm{aSMB}(\mathrm{t}), \mathrm{h}) + \mathrm{R}(\mathrm{d}(\mathrm{SMB}(0))/\mathrm{dz}, \mathrm{h}_0) * \mathrm{dh}(\mathrm{t}). \quad (12)$$

https://doi.org/10.5194/tc-2019-188
Preprint. Discussion started: 4 September 2019

To calculate (12), we remap the time-dependent $\mathrm{aSMB}(t,\bar{h})$ and the initial $\mathrm{d(SMB(0))/dz}$ to the time-evolving ice-sheet topography h.

From a practical point of view, the first option (remap to a fixed initial elevation and apply d(SMB)/dz(t), Eq.(10)) is much easier to achieve and has been chosen for the ISMIP6 projections (Nowicki et al., 2016; Goelzer et al., 2019). In that case, the remapping can be done offline for a given initial ice sheet geometry, instead of online in each ice sheet model. The format of data to be exchanged is the same with and without remapping: the modeller receives time-dependent aSMB(x,y,t) and d(SMB)/dz(x,y,t) and has to implement a mechanism to calculate the additional term due to elevation change from the latter.

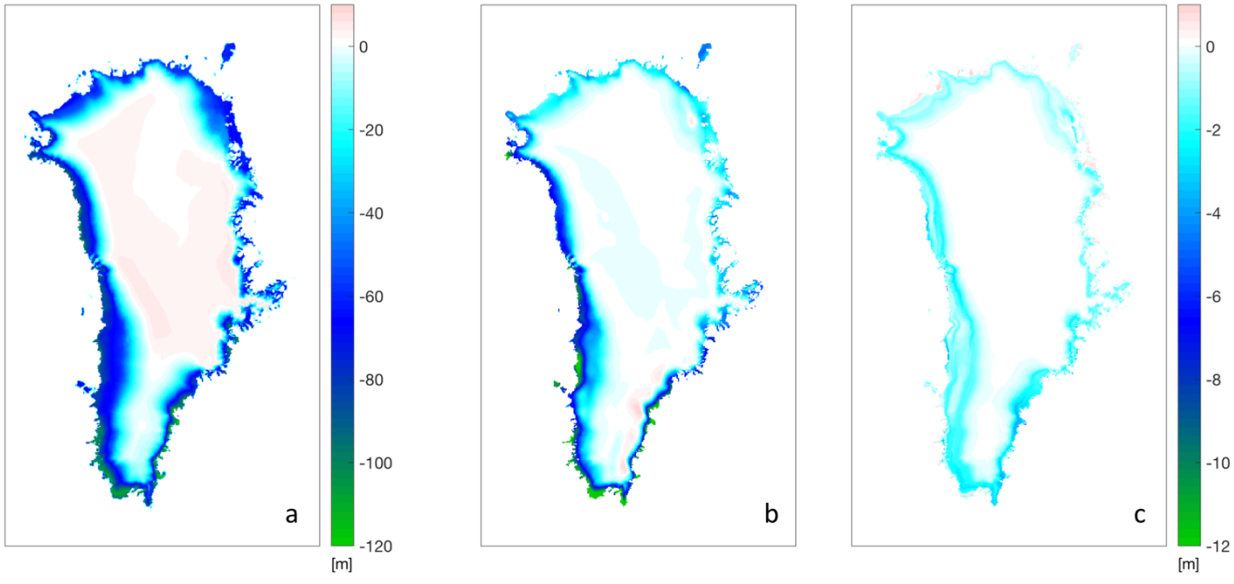

Figure 11 Total elevation change 2015-2100 due to local time-integration of aSMB with remapping to the evolving geometry (a), elevation change due to d(SMB)/dz(t) (b) and due to remapping only (c).

4.3 Application to a large ice sheet model ensemble

To illustrate the use of the proposed method for a larger group of models, we have applied the transient aSMB calculation for the modelled initial states of the initMIP-Greenland ensemble (Goelzer et al., 2018a). We use the publicly available output of the initial model states, which are provided on a common diagnostic grid (Goelzer et al., 2018b). The time-dependent aSMB of MIROC5-forced MAR (RCP8.5) is remapped to the surface elevation of the initial state of each model. The geometry is then propagated (similar to section 4.1) over the period 2015-2100 as a function of the applied SMB anomaly (no ice sheet model is used), taking the height-SMB feedback into account as described in the last section. The resulting sea-level

https://doi.org/10.5194/tc-2019-188
Preprint. Discussion started: 4 September 2019

contribution (Figure 12a) is calculated by time-integration of the aSMB assuming an ocean surface area of 361.8 × 10^6 km^2 and an ice density of 917 kg m^{-3}. Differences between models are due to differences in (initial) ice sheet extent and surface elevation. We compare this result to a control experiment, with surface elevation changes considered as above, but here the original MAR aSMB is applied without remapping (Figure 12b).

Comparison between the two cases shows that (unphysical) biases in the estimated sea-level contribution are considerably reduced, especially for the models that show a too large initial ice sheet extent and consequently a too large sea-level contribution. However, some (physical) biases remain as expected, e.g. because a larger ice sheet has a larger ablation area.

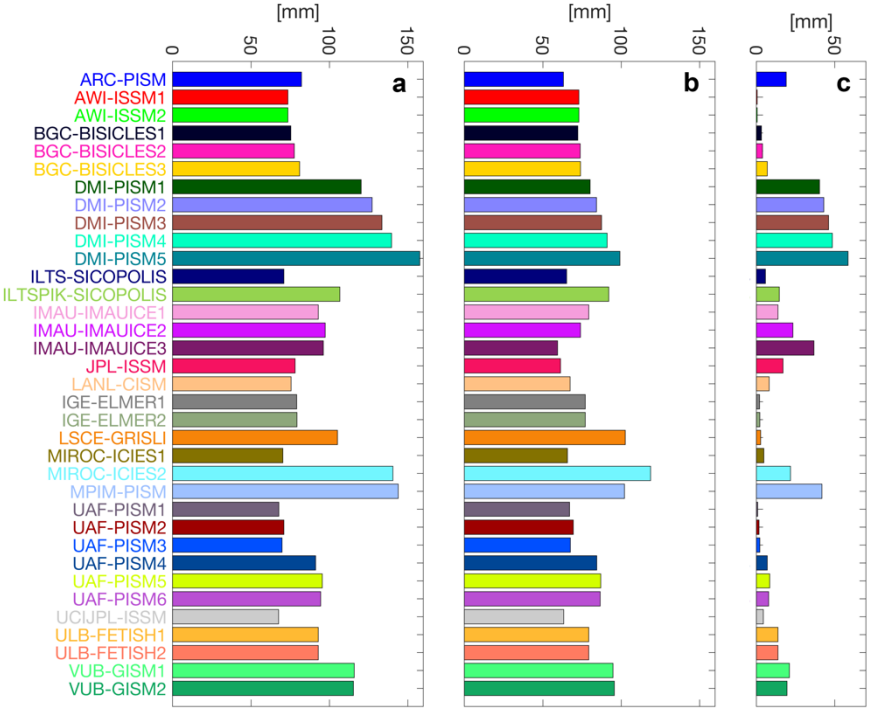

Figure 12 Sea-level contribution in 2100 derived by integrating a transient aSMB over the initial ice mask of each initMIP-Greenland model, (a) without remapping, but extension to the modelled ice sheet extent, (b) with remapping to the initial surface elevation of each individual model and (c) difference a-b.

5 Discussion and conclusions

The described method allows application of SMB anomaly forcing for a large range of different ice sheet models and addresses problems arising from differences in initial ice sheet geometry. Remapping to the same geometry closely reproduces the original aSMB, while remapping to other, modelled geometries shows patterns similar to the original, with smooth and continuous aSMB across basin divides. This shows that the method is indeed suited to record and remap the aSMB for a wide range of ice sheet geometries, while retaining the physical relationships originally represented by the data.

https://doi.org/10.5194/tc-2019-188
Preprint. Discussion started: 4 September 2019

Because the method produces a physically consistent aSMB forcing for a given ice sheet geometry, it also propagates biases in surface elevation to the SMB. This implies that for a given ice sheet geometry, biases due to a different ice sheet mask or due to elevation differences have to be accepted. In cases where the ice sheet mask is quite well matched, it may be preferred to apply aSMB without remapping to prevent propagation of small biases in surface elevation to the SMB forcing. In the initMIP-Greenland ensemble as a whole, biases due to differences in ice sheet mask were dominant, but this is not the case for each individual model. Therefore, we propose to evaluate the magnitude of the implied aSMB biases in offline calculations to decide whether remapping should be applied or not.

The main difference between our method and existing approaches of transforming the SMB to a different geometry (Franco et al., 2012; Helsen et al., 2013) is the non-locality of the remapping process, which may be described as its key feature. Like Helsen et al., (2013) and Franco et al., (2012), we assume a linear relationship between elevation and SMB for a given time and location, but that relationship it is not geographically uniform or constant in time. This means, however, that the original aSMB field is not exactly reproduced when the remapping is applied to an ice sheet with identical surface elevation, at least not for the basin delineation currently used. However, in the limit of reducing the width of the basins to individual flowlines, the reproduction of the aSMB at the original geometry should converge to the original field. Using a basin separation based on flow-lines is preferable, because they mostly follow the surface elevation gradient so the aSMB can be sampled in a continuous method that largely maintains the spatial structure. While this would increase the number of parameters that have to be fitted for each individual model geometry, it would also allow further improvement of the aSMB representation.

The ice sheet integrated mass anomaly is not conserved when remapping to a different geometry, given that a different geometry demands a different SMB forcing. It would in principle be possible to impose mass conservation on the ice sheet or even on the basin scale by comparing spatial averages of the original and remapped forcing and subtracting the difference. This would lead, however, to a spatial shift of regions where positive and negative anomalies are applied and, in the latter case, to discontinuities between neighbouring basins. Similar problems would arise for rescaling of aSMB.

We have shown how to apply the method for different ice sheet geometries, but have circumvented so far the problem of different model grids. While for ISMIP6 we have chosen to interpolate the already remapped aSMB to the native ice sheet model grids, the method could also be applied directly after interpolating the basin division and weighting to the individual ice sheet model grid. If the remapping were to be implemented in the ice sheet model itself, it could even be applied for adaptive grids that change over time.

Data availability. The basin delineation is provided as supplement to this publication. The MAR based outputs for ISMIP6 are available on ftp://climato.be/fettweis/MARv3.9/ISMIP6.

Author contribution. HG conceived the study and developed the remapping method in discussion with the other authors. HG wrote the manuscript with assistance of the other authors.

Competing interests. Xavier Fettweis is a member of the editorial board of the journal.

Acknowledgements. We would like to thank Matthew Beckley for help with the extended basin delineation and Florian Ziemen for helpful discussion of early ideas for the proposed method. We acknowledge CMIP6 and the modelling groups participating in the initMIP-Greenland experiments of ISMIP6 for sharing their data and all members of the ISMIP6 team for discussions and feedback, with particular thanks to Sophie Nowicki and Tony Payne for their leadership.

Heiko Goelzer and Brice Noël have received funding from the program of the Netherlands Earth System Science Centre (NESSC), financially supported by the Dutch Ministry of Education, Culture and Science (OCW) under Grantnr. 024.002.001. Brice Noël acknowledges additional funding from the Netherlands Organisation for Polar Research (NWO). Computational resources for the MAR simulations performed for ISMIP6 have been provided by the Consortium des Équipements de Calcul Intensif (CÉCI), funded by the Fonds de la Recherche Scientifique de Belgique (F.R.S.–FNRS) under grant no. 2.5020.11 and the Tier-1 supercomputer (Zenobe) of the Fédération Wallonie Bruxelles infrastructure funded by the Walloon Region under the grant agreement no. 1117545. This material is based in part upon work supported by the National Center for Atmospheric Research, which is a major facility sponsored by the National Science Foundation under Cooperative Agreement No. 1852977.

References

Delhasse, A., Kittel, C., Amory, C., Hofer, S., and Fettweis, X.: Brief communication: Interest of a regional climate model against ERA5 to simulate the near-surface climate of the Greenland ice sheet, The Cryosphere Discuss., 2019, 1-12, doi:10.5194/tc-2019-96, 2019.

Edwards, T. L., Fettweis, X., Gagliardini, O., Gillet-Chaulet, F., Goelzer, H., Gregory, J. M., Hoffman, M., Huybrechts, P., Payne, A. J., Perego, M., Price, S., Quiquet, A., and Ritz, C.: Effect of uncertainty in surface mass balance–elevation feedback on projections of the future sea level contribution of the Greenland ice sheet, The Cryosphere, 8, 195-208, doi:10.5194/tc-8-195-2014, 2014a.

Edwards, T. L., Fettweis, X., Gagliardini, O., Gillet-Chaulet, F., Goelzer, H., Gregory, J. M., Hoffman, M., Huybrechts, P., Payne, A. J., Perego, M., Price, S., Quiquet, A., and Ritz, C.: Probabilistic parameterisation of the surface mass balance–elevation feedback in regional climate model simulations of the Greenland ice sheet, The Cryosphere, 8, 181-194, doi:10.5194/tc-8-181-2014, 2014b.

Eyring, V., Bony, S., Meehl, G. A., Senior, C. A., Stevens, B., Stouffer, R. J., and Taylor, K. E.: Overview of the Coupled Model Intercomparison Project Phase 6 (CMIP6) experimental design and organization, Geosci. Model Dev., 9, 1937-1958, doi:10.5194/gmd-9-1937-2016, 2016.

https://doi.org/10.5194/tc-2019-188
Preprint. Discussion started: 4 September 2019

Fettweis, X., Franco, B., Tedesco, M., van Angelen, J. H., Lenaerts, J. T. M., van den Broeke, M. R., and Gallée, H.: Estimating the Greenland ice sheet surface mass balance contribution to future sea level rise using the regional atmospheric climate model MAR, The Cryosphere, 7, 469-489, doi:10.5194/tc-7-469-2013, 2013.

Franco, B., Fettweis, X., Lang, C., and Erpicum, M.: Impact of spatial resolution on the modelling of the Greenland ice sheet surface mass balance between 1990–2010, using the regional climate model MAR, The Cryosphere, 6, 695-711, doi:10.5194/tc-6-695-2012, 2012.

Goelzer, H., Huybrechts, P., Fürst, J. J., Andersen, M. L., Edwards, T. L., Fettweis, X., Nick, F. M., Payne, A. J., and Shannon, S. R.: Sensitivity of Greenland ice sheet projections to model formulations, J. Glaciol., 59, 733–749, doi:10.3189/2013JoG12J182, 2013.

Goelzer, H., Nowicki, S., Edwards, T., Beckley, M., Abe-Ouchi, A., Aschwanden, A., Calov, R., Gagliardini, O., Gillet-Chaulet, F., Golledge, N. R., Gregory, J., Greve, R., Humbert, A., Huybrechts, P., Kennedy, J. H., Larour, E., Lipscomb, W. H., Le clec'h, S., Lee, V., Morlighem, M., Pattyn, F., Payne, A. J., Rodehacke, C., Rückamp, M., Saito, F., Schlegel, N., Seroussi, H., Shepherd, A., Sun, S., van de Wal, R., and Ziemen, F. A.: Design and results of the ice sheet model initialisation experiments initMIP-Greenland: an ISMIP6 intercomparison, The Cryosphere, 12, 1433-1460, doi:10.5194/tc-12-1433-2018, 2018a.

Goelzer, H., Nowicki, S., Edwards, T., Beckley, M., Abe-Ouchi, A., Aschwanden, A., Calov, R., Gagliardini, O., Gillet-Chaulet, F., Golledge, N. R., Gregory, J., Greve, R., Humbert, A., Huybrechts, P., Kennedy, J. H., Larour, E., Lipscomb, W. H., Le clec'h, S., Lee, V., Morlighem, M., Pattyn, F., Payne, A. J., Rodehacke, C., Rückamp, M., Saito, F., Schlegel, N., Seroussi, H., Shepherd, A., Sun, S., van de Wal, R., and Ziemen, F. A.: Results of the ice sheet model initialisation experiments initMIP-Greenland: an ISMIP6 intercomparison, 10.5281/zenodo.1173088, 2018b.

Goelzer, H., Nowicki, S., Abe-Ouchi, A., Aschwanden, A., Barthel, A. M., Calov, R., Choi, Y., Cornford, S., Cuzzone, J. K., Dumas, C., Edwards, T., Felikson, D., Fettweis, X., Gillet-Chaulet, F., Golledge, N. R., Gregory, J., Greve, R., Humbert, A., Huybrechts, P., Kennedy, J. H., Larour, E., Lipscomb, W. H., Little, C., Le clec'h, S., Lee, V., Leguy, G., Lowry, D., Martin, D., Morlighem, M., Nias, I., Pattyn, F., Payne, A. J., Quiquet, A., Rückamp, M., Schlegel, N., Seroussi, H., Shepherd, A., Simon, E., Slater, D., Straneo, F., Sun, S., Tarasov, L., and van de Wal, R.: The future sea-level contribution of the Greenland ice sheet: a multi-model ensemble study of ISMIP6, in prep., 2019.

Helsen, M. M., van de Berg, W. J., van de Wal, R. S. W., van den Broeke, M. R., and Oerlemans, J.: Coupled regional climate-ice-sheet simulation shows limited Greenland ice loss during the Eemian, Clim. Past., 9, 1773-1788, doi:10.5194/cp-9-1773-2013, 2013.

IPCC: Climate Change 2013: The Physical Science Basis. Contribution of Working Group I to the Fifth Assessment Report of the Intergovernmental Panel on Climate Change edited by: Stocker, T. F., Qin, D., Plattner, G.-K., Tignor, M., Allen, S. K., Boschung, J., Nauels, A., Xia, Y., Bex, V., and Midgley, P. M., Cambridge University Press, Cambridge, United Kingdom and New York, NY, USA, 2013.

https://doi.org/10.5194/tc-2019-188
Preprint. Discussion started: 4 September 2019

Le clec'h, S., Charbit, S., Quiquet, A., Fettweis, X., Dumas, C., Kageyama, M., Wyard, C., and Ritz, C.: Assessment of the Greenland ice sheet–atmosphere feedbacks for the next century with a regional atmospheric model coupled to an ice sheet model, The Cryosphere, 13, 373-395, doi:10.5194/tc-13-373-2019, 2019.

Mouginot, J., Rignot, E., Bjørk, A. A., van den Broeke, M., Millan, R., Morlighem, M., Noël, B., Scheuchl, B., and Wood, M.: Forty-six years of Greenland Ice Sheet mass balance from 1972 to 2018, Proceedings of the National Academy of Sciences, 116, 9239, doi:10.1073/pnas.1904242116, 2019.

Noël, B., van de Berg, W. J., Machguth, H., Lhermitte, S., Howat, I., Fettweis, X., and van den Broeke, M. R.: A daily, 1 km resolution data set of downscaled Greenland ice sheet surface mass balance (1958–2015), The Cryosphere, 10, 2361-2377, doi:10.5194/tc-10-2361-2016, 2016.

Nowicki, S. M. J., Payne, A., Larour, E., Seroussi, H., Goelzer, H., Lipscomb, W., Gregory, J., Abe-Ouchi, A., and Shepherd, A.: Ice Sheet Model Intercomparison Project (ISMIP6) contribution to CMIP6, Geosci. Model Dev., 9, 4521-4545, doi:10.5194/gmd-9-4521-2016, 2016.

Seroussi, H., Nowicki, S., Simon, E., Abe-Ouchi, A., Albrecht, T., Brondex, J., Cornford, S., Dumas, C., Gillet-Chaulet, F., Goelzer, H., Golledge, N. R., Gregory, J. M., Greve, R., Hoffman, M. J., Humbert, A., Huybrechts, P., Kleiner, T., Larour, E., Leguy, G., Lipscomb, W. H., Lowry, D., Mengel, M., Morlighem, M., Pattyn, F., Payne, A. J., Pollard, D., Price, S. F., Quiquet, A., Reerink, T. J., Reese, R., Rodehacke, C. B., Schlegel, N. J., Shepherd, A., Sun, S., Sutter, J., Van Breedam, J., van de Wal, R. S. W., Winkelmann, R., and Zhang, T.: initMIP-Antarctica: an ice sheet model initialization experiment of ISMIP6, The Cryosphere, 13, 1441-1471, doi:10.5194/tc-13-1441-2019, 2019.

Shepherd, A., Ivins, E. R., A, G., Barletta, V. R., Bentley, M. J., Bettadpur, S., Briggs, K. H., Bromwich, D. H., Forsberg, R., Galin, N., Horwath, M., Jacobs, S., Joughin, I., King, M. A., Lenaerts, J. T. M., Li, J., Ligtenberg, S. R. M., Luckman, A., Luthcke, S. B., McMillan, M., Meister, R., Milne, G., Mouginot, J., Muir, A., Nicolas, J. P., Paden, J., Payne, A. J., Pritchard, H., Rignot, E., Rott, H., Sørensen, L. S., Scambos, T. A., Scheuchl, B., Schrama, E. J. O., Smith, B., Sundal, A. V., van Angelen, J. H., Van De Berg, W. J., Van Den Broeke, M. R., Vaughan, D. G., Velicogna, I., Wahr, J., Whitehouse, P. L., Wingham, D. J., Yi, D., Young, D., and Zwally, H. J.: A Reconciled Estimate of Ice-Sheet Mass Balance, Science, 338, 1183-1189, doi:10.1126/science.1228102, 2012.

van den Broeke, M., Box, J., Fettweis, X., Hanna, E., Noël, B., Tedesco, M., van As, D., van de Berg, W. J., and van Kampenhout, L.: Greenland Ice Sheet Surface Mass Loss: Recent Developments in Observation and Modeling, Current Climate Change Reports, 3, 345-356, doi:10.1007/s40641-017-0084-8, 2017.

Watanabe, M., Suzuki, T., O'ishi, R., Komuro, Y., Watanabe, S., Emori, S., Takemura, T., Chikira, M., Ogura, T., Sekiguchi, M., Takata, K., Yamazaki, D., Yokohata, T., Nozawa, T., Hasumi, H., Tatebe, H., and Kimoto, M.: Improved Climate Simulation by MIROC5: Mean States, Variability, and Climate Sensitivity, J. Clim., 23, 6312-6335, doi:10.1175/2010JCLI3679.1, 2010.

Zwally, H. J., Giovinetto, M. B., Beckley, M. A., and Saba, J. L.: Antarctic and Greenland Drainage Systems, GSFC Cryospheric Sciences Laboratory, http://icesat4.gsfc.nasa.gov/cryo_data/ant_grn_drainage_systems.php, 2012.